JOURNAL OF MATERIALS SCIENCE 30 (1995) 5750–5754

Bending of shape-memory alloy-reinforced composite beam

GUOJUN SUN
School of Civil Engineering and Mechanics, Shanghai Jiao Tong University, Shanghai 200030, People's Republic of China
C. T. SUN
Department of Aerospace Engineering, Mechanics and Engineering Science, University of Florida, Gainesville, FL 32611, USA

Based on the one-dimensional thermo-mechanical constitutive relation of a shape-memory alloy (SMA) in which the dependence of the elastic modulus of SMA upon the martensite fraction is considered, a constitutive relation for the bending of a composite beam with eccentrically embedded SMA wires has been developed. The deflection–temperature relation upon heating and cooling has been analysed for the SMA-reinforced composite beam.

1. Introduction

The shape-memory alloy has attracted wide attention during the past decades due to its unique shape-memory effect (SME). It has been successfully used in many engineering as well as medical applications, such as tube connectors, joint rivets, satellite antenna, actuators in automatic control system and medical appliances in orthodontia and orthopaedic surgery. Only in recent years, however, has a further important application of SMA been found because it is a typical "smart material" as proposed by Rogers and Robertshaw [1]. The SMA, as well as other smart materials, such as optical fibres, electro-rheological fluids and piezoelectric materials, can be attached to or embedded in conventional fibre-reinforced composites or isotropic materials (metals or plastics) to act as a sensor or actuator. One of the prospective applications of SMA-reinforced composites is the active vibration control of large flexible aerospace and space structures. Thus it would be beneficial to know explicitly the constitutive relations between applied forces, deformation and temperature of SMA-reinforced structural components before the active control of their dynamic responses are investigated.

In a previous study [2], we developed a thermo-mechanical constitutive relation for SMA-reinforced lamina in which the dependence of the elastic modulus of SMA upon the martensite fraction is taken into account. The constitutive relation between the applied moment, the curvature and temperature for a composite beam with eccentrically embedded SMA wires has been further developed and its free bending due to heating and cooling has been analysed in the present study based on the same consideration.

2. Tensile behaviour of the SMA wire

Before the behaviour of SMA-reinforced composites is analysed, it is necessary to give a mathematical description of the tensile behaviour of a pure SMA wire. The uniaxial thermo-mechanical relation of SMA during the course of stress-induced martensitic transformation or the reverse transformation, has been given by Tanaka [3]

$$\dot{\sigma}_a = D\dot{\varepsilon}_a + \theta\dot{T} + \Omega\dot{\xi} \quad (1)$$

where σ_a and ε_a are the stress and the strain of SMA, D, θ and Ω are elastic modulus, thermo-coefficient and phase-transformation coefficient of SMA, respectively. ξ is the martensite fraction ($0 \le \xi \le 1$), T is the temperature. The elastic modulus, D, is in general a function of temperature, T, and martensite fraction, ξ. In most of the previous research [3,4] D was treated as a constant throughout the process. However, the elastic modulus of SMA in the martensite phase is often much less than that in the austenite phase. The elastic modulus of 55-NiTinol in the austenite phase, for example, is more than three times as high as that in the martensite phase. As in the previous study [2], the present study also assumes that $D(\xi)$ is a function of ξ such that

$$D(\xi) = \frac{D_A - D_M}{2}[\cos(\xi\pi) + 1] + D_M \quad (2)$$

where D_M and D_A are elastic modulus of SMA when in the martensite phase ($\xi = 1$) and in the austenite phase ($\xi = 0$), respectively.

Equation 1 can then be written in the following differential form

$$D(\xi)\mathrm{d}\varepsilon_a = \mathrm{d}\sigma_a - \Omega\mathrm{d}\xi - \theta\mathrm{d}T \quad (3)$$

TABLE I. Material constants for SMA

D_A (MPa)	D_M (MPa)	Ω (MPa)	θ (MPa °C^{-1})	M_f (°C)	M_s (°C)	A_s (°C)	A_f (°C)	C_M (MPa °C^{-1})	C_A (MPa °C^{-1})
75.9×10^3	24.1×10^3	−700	0.1	−30	0	10	40	2.5	2.5

Liang and Rogers [4] suggested that the dependence of martensite fraction, ξ, upon temperature, T, and stress, σ_a, of SMA can be described by a cosine function. During the course of the phase transformation from martensite to austenite, ξ is given by

$$\xi = \frac{1}{2}\xi_M\{\cos[a_A(T - A_S) - b_A\sigma_a] + 1\} \quad (4)$$

and during the course of martensitic transformation

$$\xi = \frac{1}{2}(1 - \xi_A)\cos[a_M(T - M_f) - b_M\sigma_a] + \frac{1}{2}(1 + \xi_A) \quad (5)$$

where the material coefficients are

$$a_A = \frac{\pi}{A_f - A_s} \quad (6a)$$

$$a_M = \frac{\pi}{M_s - M_f} \quad (6b)$$

$$b_A = \frac{a_A}{C_A} \quad (6c)$$

$$b_M = \frac{a_M}{C_M} \quad (6d)$$

where A_s, A_f, M_s and M_f are the austenite and martensite start and finish temperatures of the SMA under stress-free conditions; respectively. C_A and C_M are SMA material constants related to stress-induced phase transformation. ξ_M and ξ_A are initial martensite fractions when the M → A or the A → M transformation starts from a state which has mixed martensite and austenite phases.

As demonstrated elsewhere [2], the uniaxial thermo-mechanical constitutive relation of SMA can be expressed as

$$D(\xi)\mathrm{d}\varepsilon_a = \left(1 - \Omega\frac{\partial\xi}{\partial\sigma_a}\right)\mathrm{d}\sigma_a - \left(\theta + \Omega\frac{\partial\xi}{\partial T}\right)\mathrm{d}T \quad (7)$$

where the partial differential of ξ with respect to σ_a and T is given by

$$\frac{\partial\xi}{\partial\sigma_a} = \frac{1}{2}\xi_M b_A \sin[a_A(T - A_s) - b_A\sigma_a] \quad (8a)$$

$$\frac{\partial\xi}{\partial T} = -\frac{1}{2}\xi_M a_A \sin[a_A(T - A_s) - b_A\sigma_a] \quad (8b)$$

for the transformation from martensite to austenite, and

$$\frac{\partial\xi}{\partial\sigma_a} = \frac{1}{2}(1 - \xi_A)b_M \sin[a_M(T - M_f) - b_M\sigma_a] \quad (9a)$$

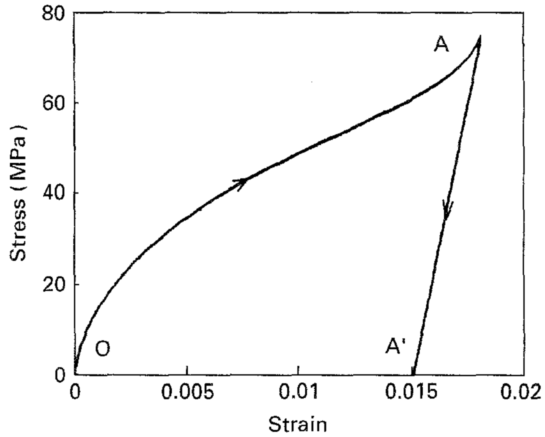

Figure 1 Stress–strain relation of a SMA wire under $T = 0$° C.

$$\frac{\partial\xi}{\partial T} = -\frac{1}{2}(1 - \xi_A)a_M \sin[a_M(T - M_f) - b_M\sigma_a] \quad (9b)$$

for the transformation from austenite to martensite.

Under constant temperature, Equation 7 becomes an ordinary differential equation because $\mathrm{d}T = 0$. The relation of stress, σ_a, and strain, ε_a, for SMA can be obtained by numerical integration such as the Runga–Kutta method. The material constants of the SMA are assumed and are listed in Table I.

Fig. 1 depicts the stress–strain relation of the SMA subjected to tensile stress under constant temperature ($T = 0$ °C). Initially the SMA is assumed in pure austenite phase ($\xi = 0$). The tensile stress causes martensite transformation and a large strain results from this phase transformation. The SMA is unloaded from point A when the stress reaches 75 MPa, and the martensite fraction ξ reaches 1. The straight line AA′ depicts that the unloading process is only an elastic recovery with the modulus in martensite phase $D_M = 24.1$ GPa. The "residual strain" remaining at zero stress can be recovered by heating the SMA. In Fig. 2 the stress–strain relation of the SMA when $T = 10$ °C is presented. Initially the SMA is also assumed to be in pure austenite phase ($\xi = 0$). Stage OA describes the elastic deformation of SMA in the austenite phase with elastic modulus $D_A = 75.9$ GPa. The stress-induced martensite transformation is started at point A and the strain increases rapidly. At point B the stress of the SMA is 80 MPa and the martensite fraction ξ is 0.83. The straight line BB′ shows that the elastic unloading starts from a state with mixed austenite and martensite phases. The modulus of this state can be obtained from Equation 2, that is, $D = 27.7$ GPa. It is found that the curves shown in Figs 1 and 2 are quite similar to the curves of experimental results reported in the literature.

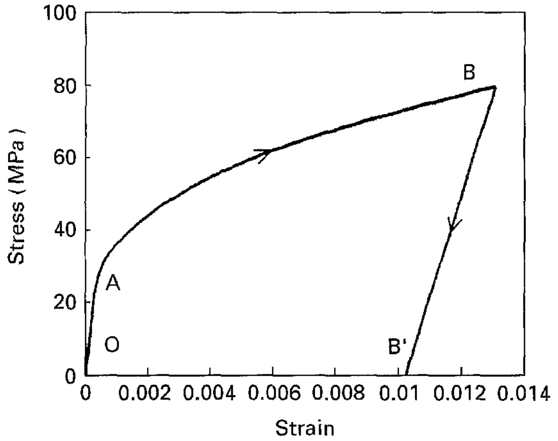

Figure 2 Stress–strain relation of a SMA wire under $T = 10°$ C.

3. Bending of the SMA-reinforced composite beam

The matrix in which SMA wires are embedded may be either conventional fibre-reinforced composites such as glass/epoxy or graphite/epoxy, or isotropic materials, such as metals or plastics. In the following, the stress and the strain of the matrix in the SMA wire's direction (axial direction) are denoted as σ_m and ε_m, the elastic modulus and the thermal expansion coefficient in the same direction are denoted as E_m and α_m, the volume fraction of the SMA wires and the matrix are denoted as V_a and V_m, respectively. If the SMA wires are elongated at a relatively low temperature, as depicted in Figs 1 and 2, a certain "residual" strain will be retained. As shown in Fig. 3, the pre-elongated SMA wires are assumed to be eccentrically embedded in a beam. It is expected that the beam will bend when heating, due to the contraction of the SMA wires during austenite phase transformation. For rectangular beam with height, h, width, b, and length, L, as shown in Fig. 4, the eccentricity parameter, e, is defined as the distance between the middle surface O′O″ and the neutral surface Ox where the axial strain is zero when bending. For simplicity of analysis, the SMA wires which are embedded below the middle surface are assumed to be a layer with height, g, and width, b. The distance between the middle surface and the top of this layer is h_1 and that between the bottom of this layer and the lower surface of the beam is h_2. The cross-sectional region of the matrix above and below the SMA layer are denoted as Ω_1 and Ω_2, respectively. There are three independent variables, namely moment M, curvature of the beam $k = 1/\rho$ (ρ is the radius of curvature), and temperature, T. The axial strain at the surface with ordinate y can be written as

$$\varepsilon = \frac{y}{\rho} \tag{10}$$

The axial equilibrium condition of stress resultants $\Sigma F_x = 0$ can be written as

$$\int_{\Omega_1} \sigma_m b\,dy + \int_{\Omega_2} \sigma_m b\,dy + \sigma_a g b = 0 \tag{11}$$

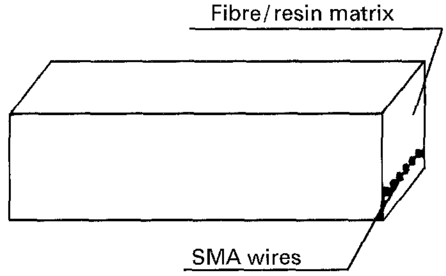

Figure 3 SMA-reinforced beam.

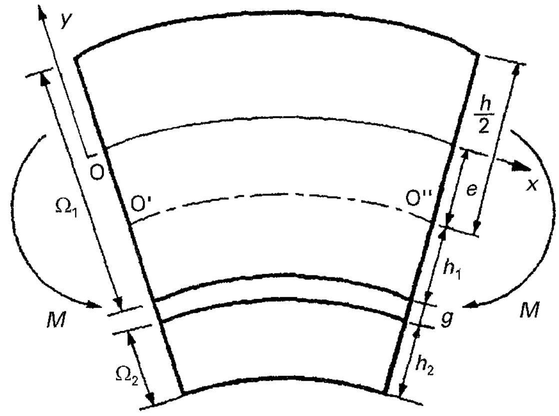

Figure 4 Geometry of the SMA-reinforced beam.

From the constitutive relation for the matrix, we have

$$\sigma_m = (\varepsilon_m - \alpha_m \Delta T)E_m = (ky - \alpha_m \Delta T)E_m \tag{12}$$

Substituting Equation 12 into Equation 11 and integrating leads to

$$(gC_2 - C_1 e)k = \alpha_m \Delta T C_1 - \frac{g}{E_m}\sigma_a \tag{13}$$

Then the stress of the embedded SMA can be written as

$$\sigma_a = \frac{g}{E_m}[\alpha_m \Delta T C_1 + (C_1 e - gC_2)k] \tag{14}$$

where $C_1 = h - g$, $C_2 = \frac{1}{2}g + h$. Equation 13 can be written in the following differential form

$$\frac{g}{E_m}d\sigma_a - kC_1 de = \alpha_m C_1 dT + (C_1 e - gC_2)dk \tag{15}$$

The strain of SMA can be written as

$$\begin{aligned}\varepsilon_a &= \frac{y_a}{\rho}\\ &= ky_a = -(e + C_2)k\end{aligned} \tag{16}$$

It is noted that the variation of the strain, ε_a, with respect to y is neglected here for simplicity. This approximation is acceptable because the volume fraction of SMA is assumed to be small. Differentiation of Equation 16 leads to

$$d\varepsilon_a = -[k\,de + (e + C_2)dk] \tag{17}$$

Eliminating $d\varepsilon_a$ from Equations 7 and 17 leads to

$$\left(1-\Omega\frac{\partial\xi}{\partial\sigma_a}\right)d\sigma_a + D(\xi)k\,de = -D(\xi)(e+C_2)\,dk + \left(\theta+\Omega\frac{\partial\xi}{\partial\sigma_a}\right)dT \quad (18)$$

Equations 15 and 18 are two simultaneous equations for the quantities $d\sigma_a$ and de. The expression for de can be written as

$$de = \left[\frac{-D(\xi)kg}{E_m} - \left(1-\Omega\frac{\partial\xi}{\partial\sigma_a}\right)kC_1\right]^{-1} \times\left\{\left[\left(1-\Omega\frac{\partial\xi}{\partial\sigma_a}\right)(C_1e-gC_2) + \frac{gD(\xi)}{E_m}(e+C_2)\right]dk + \left[\left(1-\Omega\frac{\partial\xi}{\partial\sigma_a}\right)\alpha_m C_1 - \frac{gD(\xi)}{E_m}\left(\theta+\Omega\frac{\partial\xi}{\partial\sigma_a}\right)\right]dT\right\} \quad (19)$$

The equilibrium of moment about the z-axis (not shown) for the beam $\Sigma M = 0$ can be written in the form

$$M = \int_{\Omega_1}\sigma_m yb\,dy + \int_{\Omega_2}\sigma_m yb\,dy + \sigma_a y_a gb \quad (20)$$

Substituting Equations 10, 12 and 15 into Equation 20, we obtain

$$-C_2khe + \left(C_2^2 g - \frac{C_3}{3}\right)k - \alpha_m\Delta TC_2h - \frac{M}{bE_m} = 0 \quad (21a)$$

where

$$C_3 = \frac{1}{4}(g^3 + 3h_1^2 g + 3h_1 g_2 - h^3) \quad (21b)$$

The expression for eccentricity, e, can be written as

$$e = \frac{[C_2^2 g - (C_3/3)]k - \alpha_m\Delta TC_2h - (M/bE_m)}{C_2hk} \quad (22)$$

Differentiation of Equation 21 leads to:

$$\frac{dM}{bE_m} = \left(C_2^2 g - \frac{C_3}{3} - C_2he\right)dk - C_2h\alpha_m\,dT - C_2hk\,de \quad (23)$$

Substitution of Equation 19 into Equation 23 leads to the differential relation of M, k and T

$$\frac{dM}{bE_m} = \left\{C_2^2 g - \frac{C_3}{3} - C_2he + C_2h\left[\left(1-\Omega\frac{\partial\xi}{\partial\sigma_a}\right)(C_1e-gC_2) + \frac{gD(\xi)}{E_m}(e+C_2)\right] \times\left[\frac{gD(\xi)}{E_m} + \left(1-\Omega\frac{\partial\xi}{\partial\sigma_a}\right)C_1\right]^{-1}\right\}dk + \left\{-C_2h\alpha_m + C_2h\left[\left(1-\Omega\frac{\partial\xi}{\partial\sigma_a}\right)\alpha_m C_1 - \frac{g}{E_m}\left(\theta+\Omega\frac{\partial\xi}{\partial T}\right)\right] \times\left[\frac{g\mathrm{d}(\xi)}{E_m} + \left(1-\Omega\frac{\partial\xi}{\partial\sigma_a}\right)C_1\right]^{-1}\right\}dT \quad (24)$$

Equation 24 is the differential constitutive relation of the applied moment, M, curvature, k, and temperature, T, of the SMA-reinforced beam. In Equation 24 both $\partial\xi/\partial\sigma_a$ and $\partial\xi/\partial T$ are functions of σ_a and T, and the variables σ_a, ξ and e are all functions of k and T. Finally, Equation 24 contains only variable M, k and T and their differentials. In a process under constant temperature, Equation 24 becomes an ordinary differential equation of M and k because $dT = 0$. The relation between the moment, M, and curvature, k, can be obtained by numerical integration of this equation. In a process when the two ends of the beam are fully restrained, i.e. $dk = 0$, the relation between the moment, M, built up in the beam and temperature, T, can be obtained by integrating Equation 24. If the process is free from external load, i.e. $dM = 0$, then integration of Equation 24 leads to the relation between the curvature, k, and temperature, T. As an example, the last case will be investigated in the next section using numerical examples.

4. Results and discussion

Two types of fibre/resin matrices are considered for calculation. The SMA wires are laid parallel to the fibres of the matrices in both cases. The first type of matrix is glass/epoxy with axial modulus $E_m = E_{11} = 39.3$ GPa, and thermal expansion coefficient $\alpha_m = 6.6\times10^{-6}\,°\mathrm{C}^{-1}$. The other one is graphite/epoxy with $E_m = 146$ GPa, $\alpha_m = -1.1\times10^{-6}\,°\mathrm{C}^{-1}$. The geometry parameters of the beam are $h = b = 5$ mm, $L = 150$ mm, $h_1 = h_2 = 1.0$ mm, $g = 0.5$ mm. The volume fraction of SMA is 10%. The deflection of the middle surface of the beam, w, can be expressed as

$$w = (\rho - e)\left(\frac{\delta^2}{2} - \frac{\delta^4}{24}\right) \quad (25)$$

where $\delta = L/[2(\rho - e)]$. In Fig. 5 the deflection, w, of the beam with glass/epoxy matrix is plotted against temperature, T. The initial temperature is assumed to be $T_0 = 0\,°\mathrm{C}$, which is well below the austenite starting temperature, A_s, and the initial martensite fraction, ξ_m, is assumed to be 1.0, i.e. the SMA is in pure martensite phase. At the stage AB, the beam bends slightly because the bending is induced by inconsistency of the thermal expansions between the matrix and the SMA wires. The magnitude of deflection due to thermal expansion is small. Starting from point B, the rate of bending of the beam increases rapidly. It is seen that point B is close to the austenite starting temperature $A_s = 10\,°\mathrm{C}$. The large magnitude of

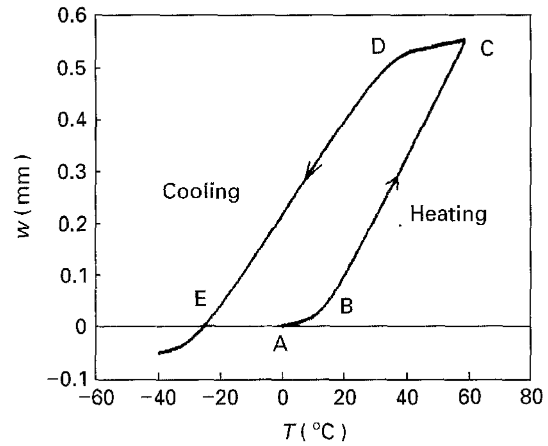

Figure 5 Deflexion–temperature relation for the SMA-reinforced beam with glass/epoxy matrix.

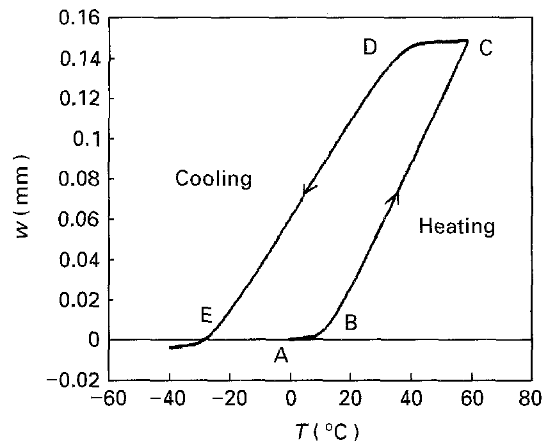

Figure 6 Deflexion–temperature relation for the SMA-reinforced beam with graphite/epoxy matrix.

bending at stage BC is caused by the contraction of SMA wires due to austenite phase transformation. The beam is assumed to be cooled down from point C when $T = 60\,^{\circ}\mathrm{C}$ and $\xi = 0.85$. The magnitude of thermal recovery at stage CD is small. The reverse transformation of SMA from austenite to martensite starts from point D. At stage DE the beam is recovered rapidly due to the martensite transformation of SMA. At this stage, the martensite transformation is caused both by decrease of temperature and by the tensile stress of SMA which is in balance with the elastic recovery force of the matrix.

Fig. 6 depicts the relation between the deflection, w, of the beam with graphite/epoxy matrix and temperature T. The starting temperature at point A is also $T_0 = 0\,^{\circ}\mathrm{C}$. Because of the high axial modulus of the graphite/epoxy matrix, the deflection of the beam is much smaller than that of the beam with glass/epoxy matrix. The trend of the variation of deflection, w, is similar to that of the beam with glass/epoxy matrix.

5. Conclusion

Besides its unique shape-memory effect, which qualifies SMA as a smart material, SMA is also a metal with good mechanical properties, such as high specific strength and high fatigue strength. In this respect, SMA has an advantage over the other smart materials, such as piezo-electric polymers, electro-rheological fluids and optical fibres. However, the disadvantage of SMA is that the reaction (stress or strain) caused by phase transformation of SMA does not proportionally relate to the input (electrical potential or current). In this study an effort has been made to develop a relation between the temperature which may be used as an intermediate variable between the input and the reaction, the applied moment and the deformation of a SMA-reinforced beam. We believe that SMA-reinforced composites have bright potential in active vibration control of aerospace and space structures.

References

1. C. A. ROGERS and H. H. ROBERTSHAW, paper presented at the ASME Winter Annual Meeting, Chicago, IL, 27 November – 2 December 1988 (ASME, New York, 1989) pp. 5–10.
2. G. SUN and C. T. SUN, *J. Mater. Sci.* **28** (1993) 6323.
3. K. TANAKA, *Res. Mech.* **8** (1986) 251.
4. C. LIANG and C. A. ROGERS, in "Proceedings of the 31st Structure, Structure Dynamics and Materials Conference" Part 1, Materials Engineering, Optimization and Design, Long Beach, CA, 2–4 April 1990 (AIAA, New York, 1990) pp. 16–28.

Received 7 April 1994
and accepted 22 June 1995